Electronic Supplementary Information

Shape-Controlled Dodecaborate Supramolecular Organic-Framework-Supported Ultrafine Trimetallic PtCoNi for Catalytic Hydrolysis of Ammonia Borane

Bin Qi,[†] Liuyi Du,[†] Fengze Yao,[†] Shuran Xu,[†] Xuefan Deng,[†] Mai Zheng,[†] Suhang He,[//] Haibo Zhang,[†‡⊥] and Xiaohai Zhou*[†‡]*

†College of Chemistry and Molecular Sciences, Wuhan University, Wuhan 430072, P. R. China

‡Engineering Research Center of Organosilicon Compounds & materials, Ministry of Education, Wuhan 430072, P. R. China

⊥National Demonstration Center for Experimental Chemistry, Wuhan University, Wuhan 430072, P. R. China

//Department of Life Sciences and Chemistry, Jacobs University Bremen, Campus Ring 1, Bremen 28759, Germany

E-mail: haibozhang1980@gmail.com (Prof. Dr. H. B. Zhang);

zxh7954@whu.edu.cn (Prof. Dr. X. H. Zhou)

Content

Figure S1. FT-IR spectrum of pure CB[5], Cs_2[*closo*-$B_{12}H_{12}$], and CB5-BOFs. 3

Figure S2. The conductivity experiment result of CB5 with different amount of $Cs_2B_{12}H_{12}$. 3

Table S1. XPS results of CB5-$Cs_2B_{12}H_{12}$ products with different feed ratio of 1 : 1, 2 : 1, 4 : 1, 6 : 1. 4

Figure S3. a), b), c), d), e), f) Views of the CB6/$B_{12}H_{12}^{2-}$ complex XRD structure. 4

Figure S4. a), b), c), d) Views of the CB7 / $B_{12}H_{11}OH^{2-}$ complex XRD structure. The CB7 component has crystallographically-imposed twofold symmetry and that the $B_{12}H_{11}OH^{2-}$ component is in a general position. 5

Figure S5. a), b), c) Views of the CB7 / $B_{12}Cl_{12}^{2-}$ complex XRD structure. The CB7 component has crystallographically-imposed twofold symmetry and that the $B_{12}Cl_{12}^{2-}$ component lies about an inversion center. 5

Figure S6. SEM images of CB5-Cs_2[*closo*-$B_{12}H_{12}$] supramolecular complex with molar ratio ([CB5]/[Cs_2[*closo*-$B_{12}H_{12}$]]) of 0.5 (a) and 0.25 (b). 6

Figure S7. EDX of single $Pt_1Co_2Ni_2$ NP supported on nanocube CB5-BOFs, showing that Pt, Co and Ni are present in both the "Area A" and "Area B". 7

Figure S8. TEM image of $Pt_1Co_{0.33}Ni_{0.33}$@nanocube BOFs. 7

Figure S9. TEM image of $Pt_1Co_{0.5}Ni_{0.5}$@nanocube BOFs. 8

Figure S10. TEM image of $Pt_1Co_1Ni_1$@nanocube BOFs. 8

Figure S11. TEM image of $Pt_1Co_3Ni_3$@nanocube BOFs. 9

Figure S12. TEM image of Pt_1Ni_2@nanocube BOFs. 9

Figure S13. TEM image of Pt_1Co_2@nanocube BOFs. 10

Figure S14. TEM image of $Ag_1Co_2Ni_2$@nanocube BOFs. 10

Figure S15. TEM image of $Pt_1Co_2Ni_2$@nanocube BOFs (a) and its enlarged image (b) after the 5th round of AB hydrolysis. 11

Figure S16. Powder XRD patterns of $Pt_1Co_2Ni_2$@nanocube BOFs before catalysis and after the 5th round of catalysis. 11

Table S2. Comparison of recent literature results for various Pt-base catalysts concerning the AB hydrolysis. 12

Reference 12

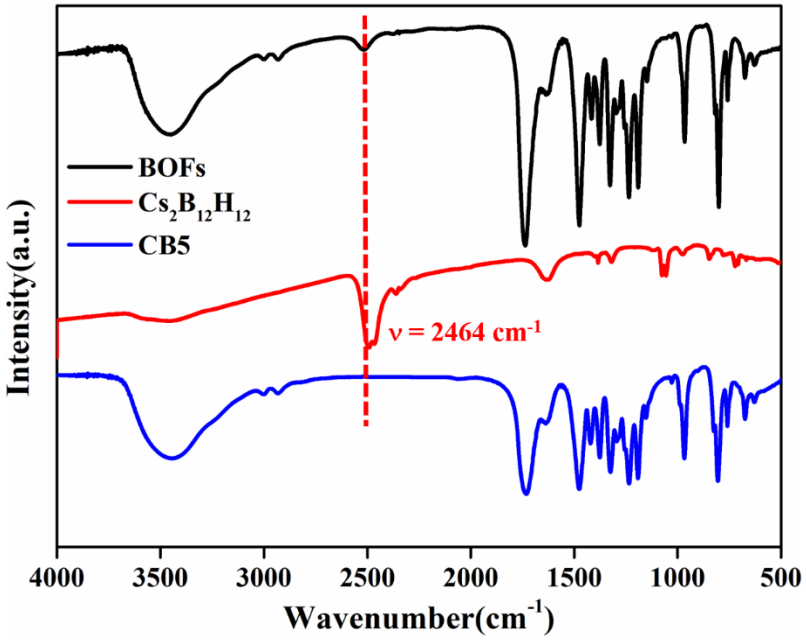

Figure S1. FT-IR spectrum of pure CB[5], Cs_2[*closo*-$B_{12}H_{12}$], and CB5-BOFs.

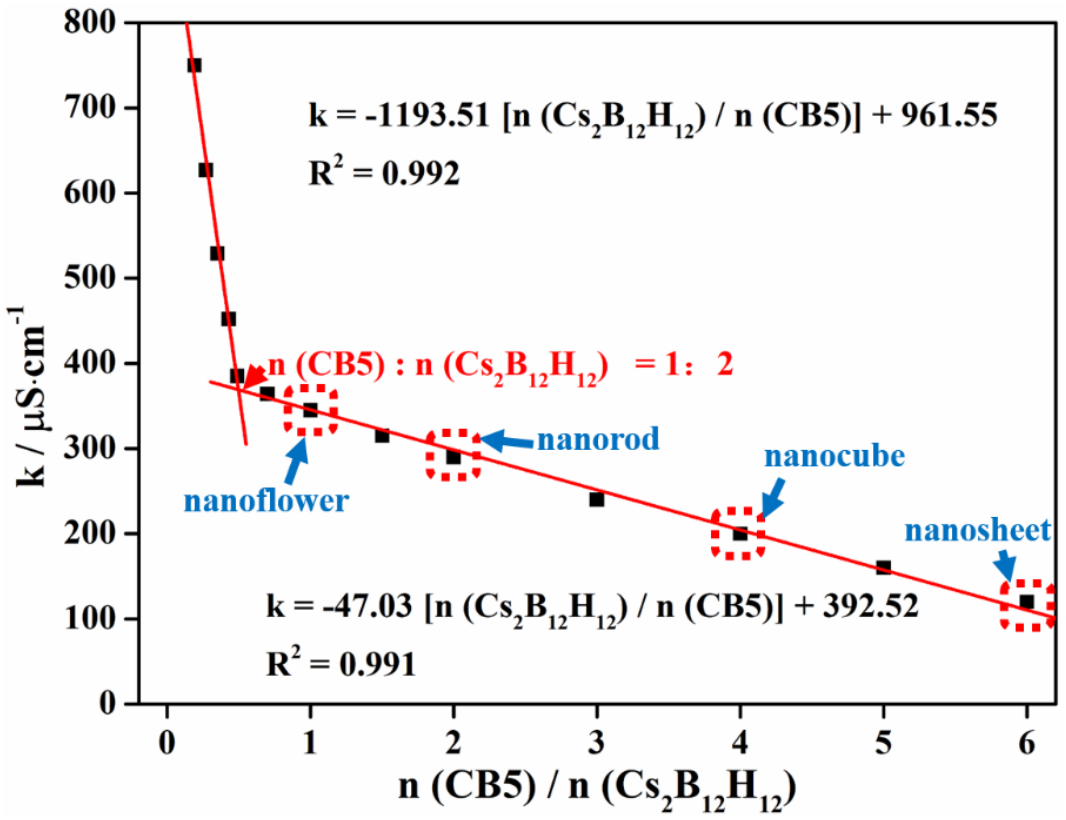

Figure S2. The conductivity experiment result of CB5 with different amount of $Cs_2B_{12}H_{12}$.

Table S1. XPS results of CB5-$Cs_2B_{12}H_{12}$ products with different feed ratio of 1 : 1, 2 : 1, 4 : 1, 6 : 1.

Feed ratio of CB5 and $Cs_2B_{12}H_{12}$	Element	Atom %	$n_{N\ atom}$ / $n_{Cs\ atom}$	*Calculation*: n_{CB5} / $n_{Cs2[B12H12]}$ (based on $n_{N\ atom}$ / $n_{Cs\ atom}$)	$n_{N\ atom}$ / $n_{B\ atom}$	*Calculation*: n_{CB5} / $n_{Cs2[B12H12]}$ (based on $n_{N\ atom}$ / $n_{B\ atom}$)
1 : 1	B 1s	11.02	11.8 : 1	1.18 : 1	1.72 : 1	1.03 : 1
	C 1s	55.76				
	Cs 3d	1.61				
	N 1s	18.97				
	O 1s	12.63				
2 : 1	B 1s	7.09	18.4 : 1	1.84 : 1	2.68 : 1	1.61 : 1
	C 1s	62.86				
	Cs 3d	1.03				
	N 1s	18.98				
	O 1s	10.03				
4 : 1	B 1s	3.29	38.6 : 1	3.86 : 1	6.09 : 1	3.66 : 1
	C 1s	64.45				
	Cs 3d	0.52				
	N 1s	20.05				
	O 1s	11.68				
6 : 1	B 1s	2.08	60.4 : 1	6.04 : 1	9.30 : 1	5.58 : 1
	C 1s	68.17				
	Cs 3d	0.32				
	N 1s	19.34				
	O 1s	10.08				

1 CB5 molecule: **20 N atoms**, 10 O atoms, 30 C atoms;
1 $Cs_2B_{12}H_{12}$ molecule: **2 Cs atoms**, **12 B atoms**.

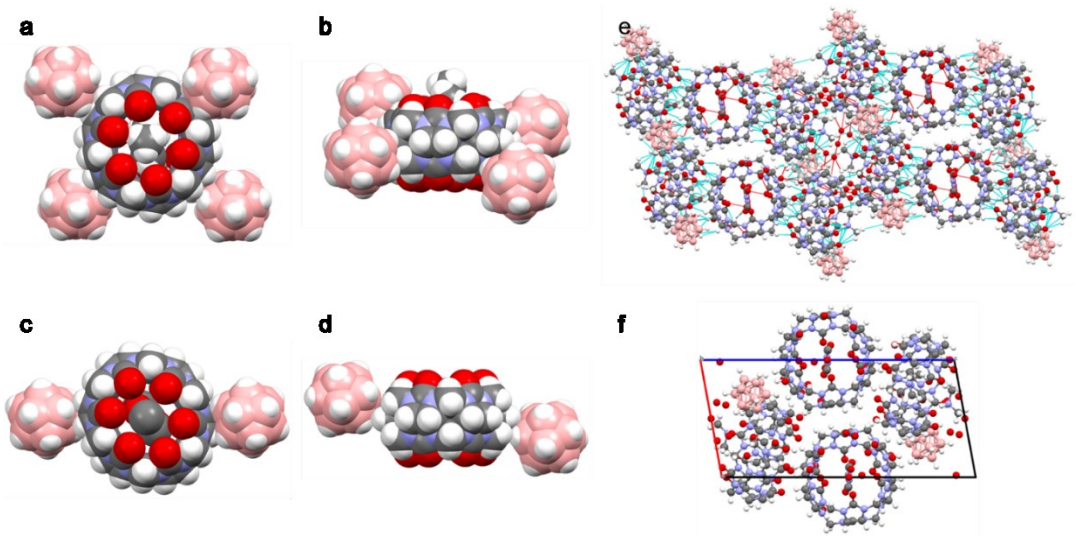

Figure S3. a), b), c), d), e), f) Views of the CB6/$B_{12}H_{12}^{2-}$ complex XRD structure.

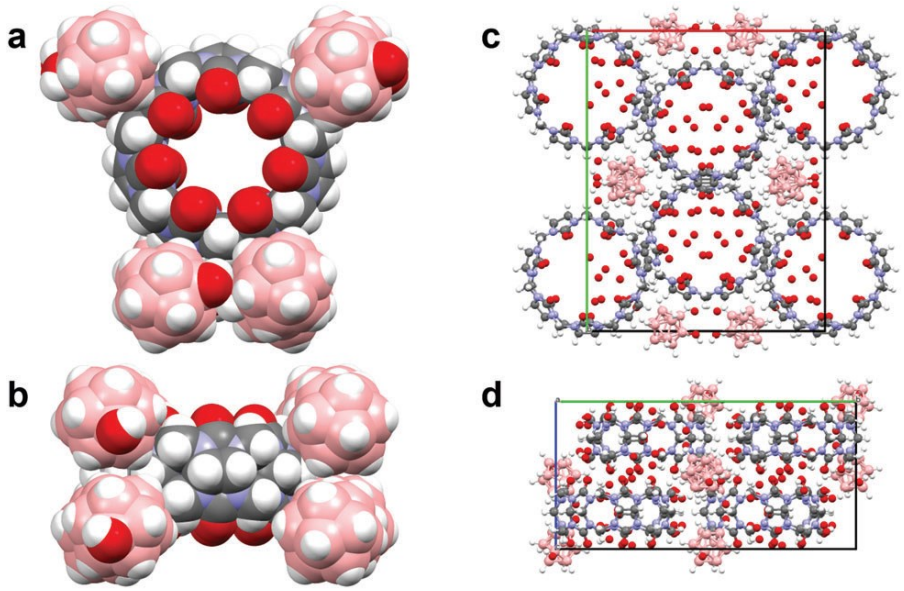

Figure S4. a), b), c), d) Views of the CB7 / $B_{12}H_{11}OH^{2-}$ complex XRD structure. The CB7 component has crystallographically-imposed twofold symmetry and that the $B_{12}H_{11}OH^{2-}$ component is in a general position.

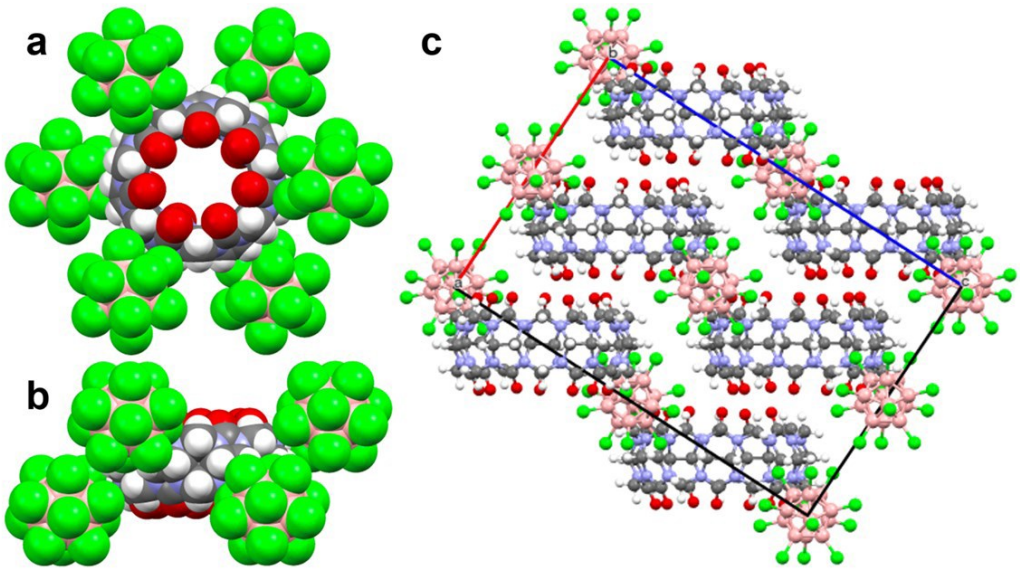

Figure S5. a), b), c) Views of the CB7 / $B_{12}Cl_{12}^{2-}$ complex XRD structure. The CB7 component has crystallographically-imposed twofold symmetry and that the $B_{12}Cl_{12}^{2-}$ component lies about an inversion center.

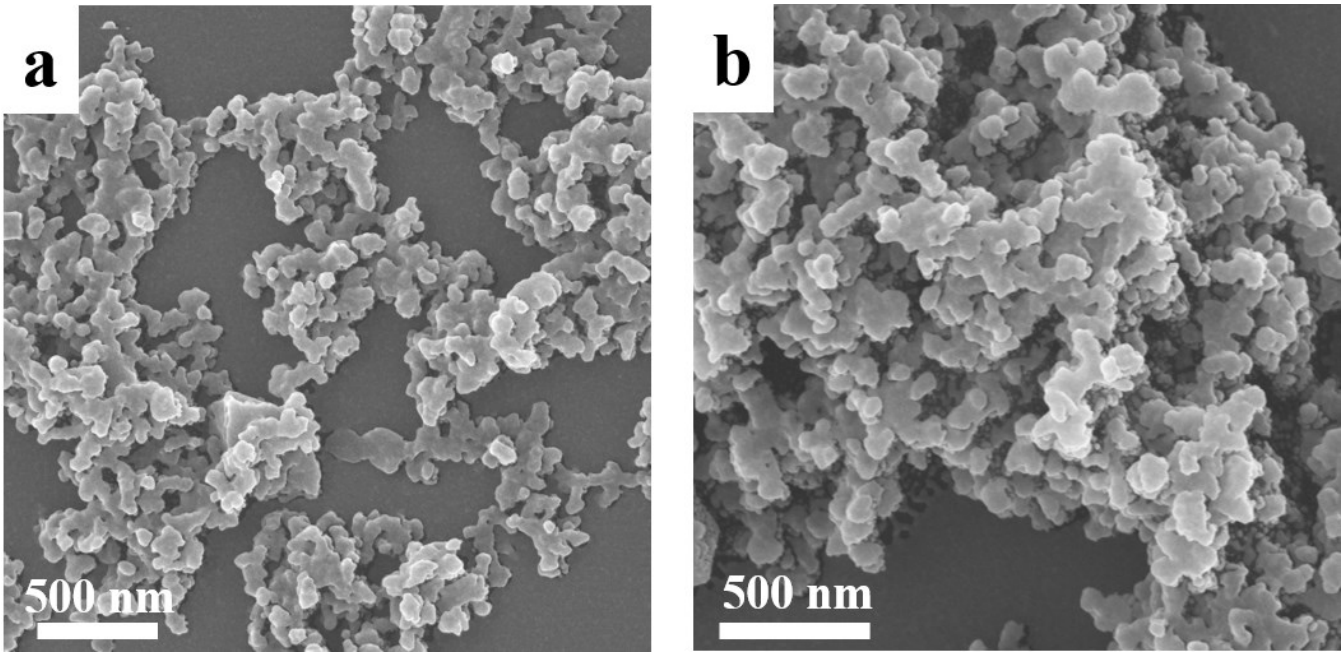

Figure S6. SEM images of CB5-Cs_2[*closo*-$B_{12}H_{12}$] supramolecular complex with molar ratio ([CB5]/[Cs_2[*closo*-$B_{12}H_{12}$]]) of 0.5 (a) and 0.25 (b).

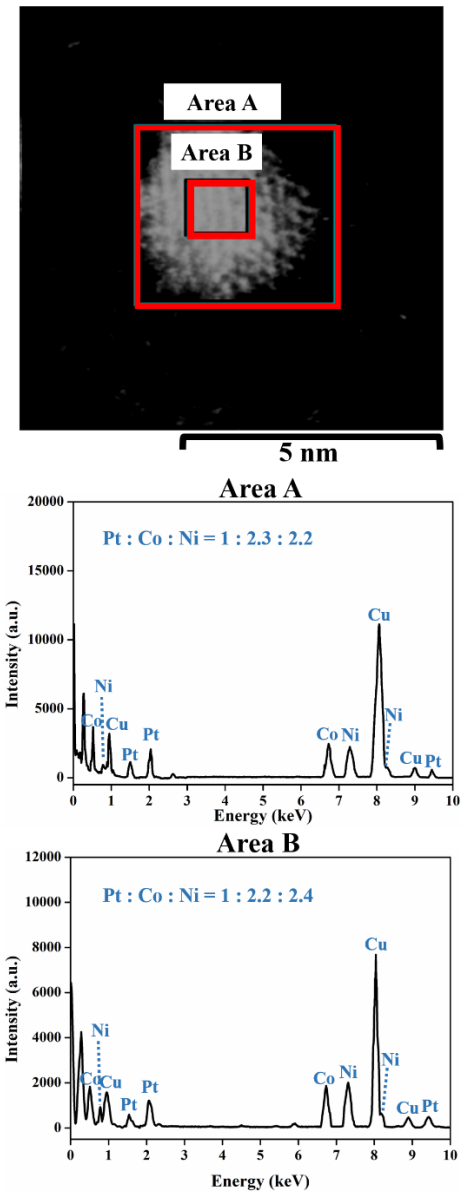

Figure S7. EDX of single $Pt_1Co_2Ni_2$ NP supported on nanocube CB5-BOFs, showing that Pt, Co and Ni are present in both the "Area A" and "Area B".

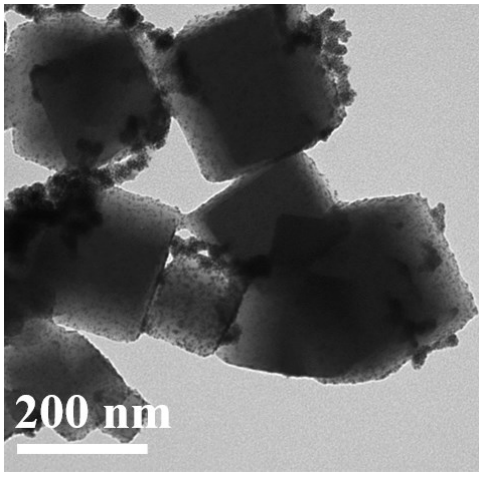

Figure S8. TEM image of $Pt_1Co_{0.33}Ni_{0.33}$@nanocube BOFs.

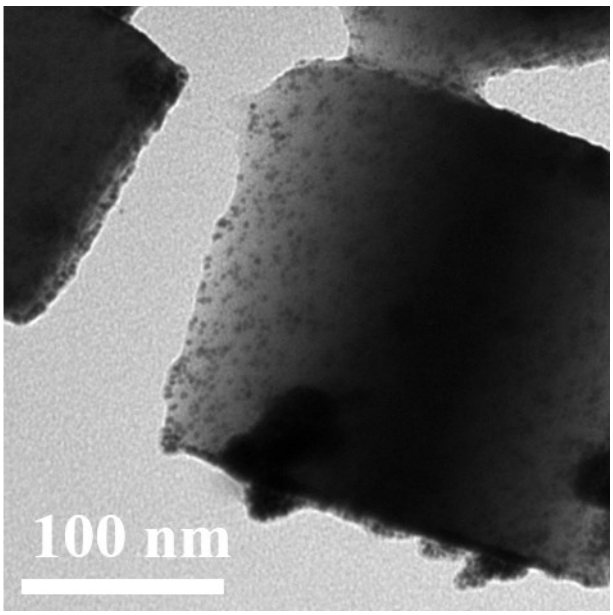

Figure S9. TEM image of $Pt_1Co_{0.5}Ni_{0.5}$@nanocube BOFs.

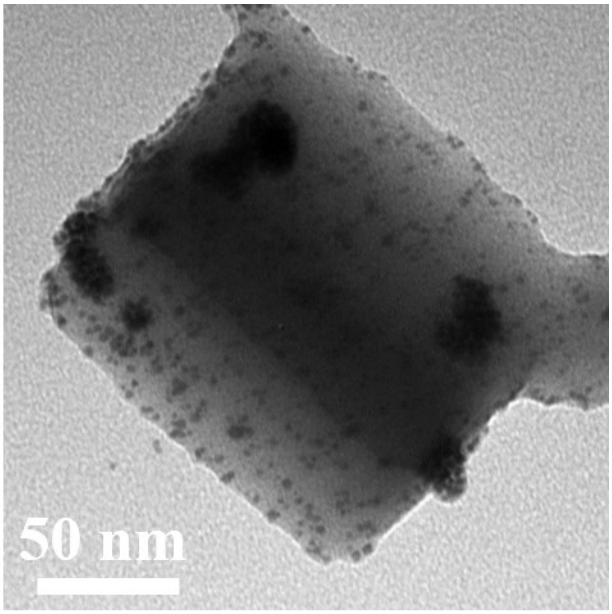

Figure S10. TEM image of $Pt_1Co_1Ni_1$@nanocube BOFs.

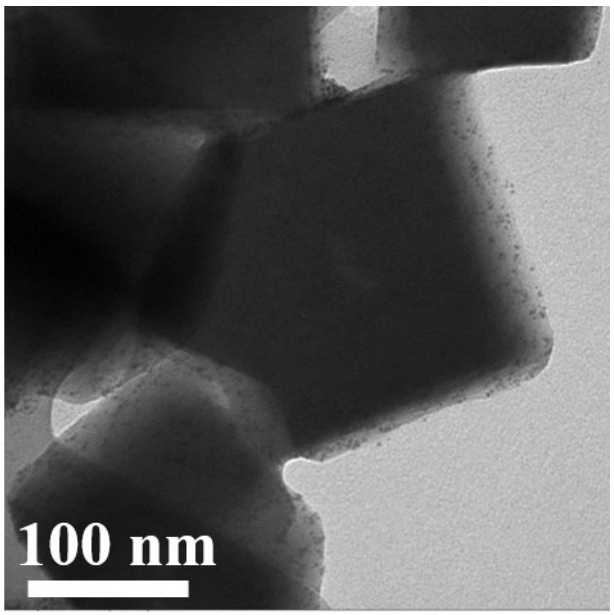

Figure S11. TEM image of $Pt_1Co_3Ni_3$@nanocube BOFs.

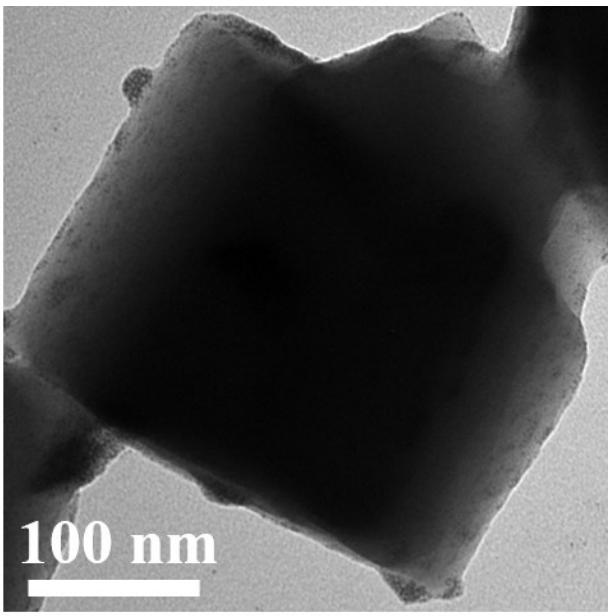

Figure S12. TEM image of Pt_1Ni_2@nanocube BOFs.

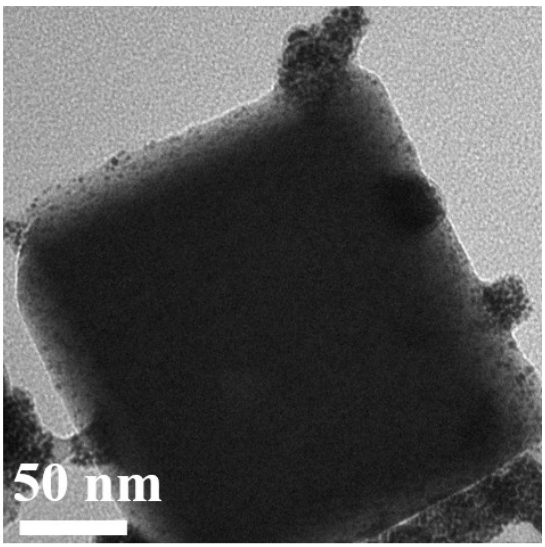

Figure S13. TEM image of Pt_1Co_2@nanocube BOFs.

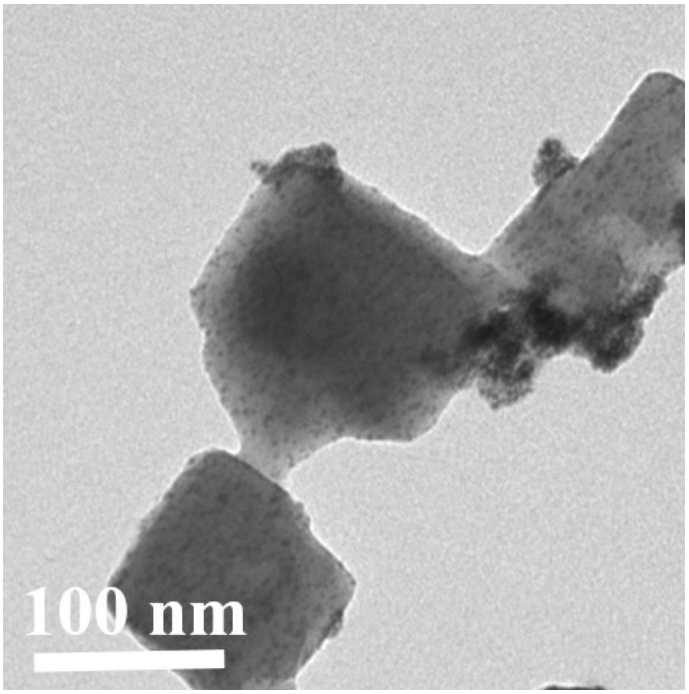

Figure S14. TEM image of $Ag_1Co_2Ni_2$@nanocube BOFs.

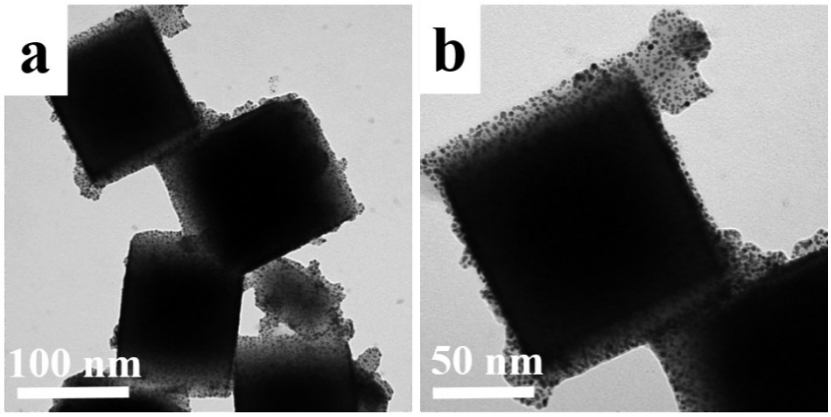

Figure S15. TEM image of $Pt_1Co_2Ni_2$@nanocube BOFs (a) and its enlarged image (b) after the 5th round of AB hydrolysis.

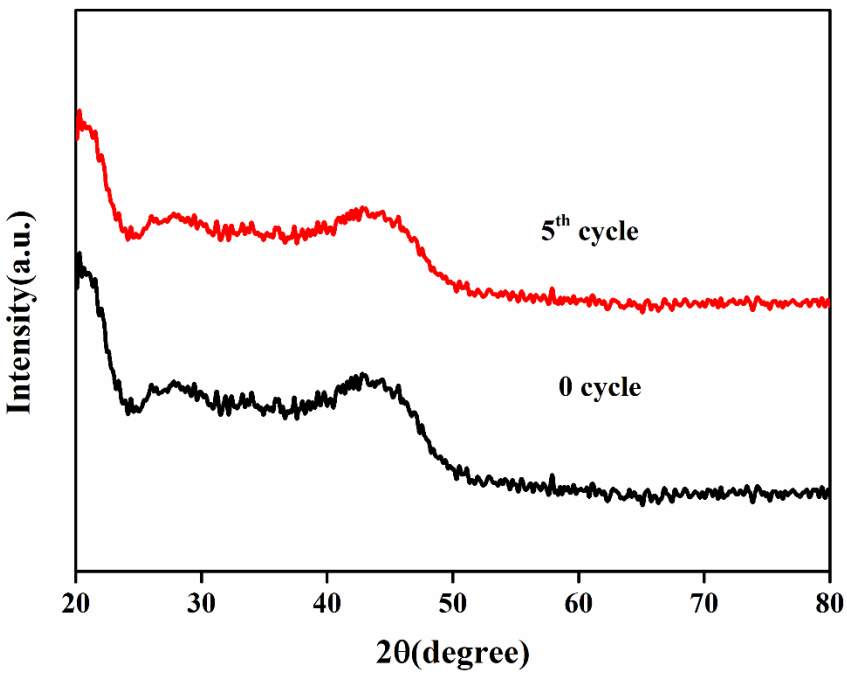

Figure S16. Powder XRD patterns of $Pt_1Co_2Ni_2$@nanocube BOFs before catalysis and after the 5th round of catalysis.

Table S2. Comparison of recent literature results for various Pt-base catalysts concerning the AB hydrolysis.

Catalyst	Temperature (°C)	Substrate	TOF (mol_{H2}·mol_{Pt}^{-1}·min^{-1})	References
PtNi@SiO_2	30	SiO_2	5.54	S1
PtRu/C	25	C	8	S2
Pt-Co	35	/	118.25	S3
$Pt_{0.68}Co_{0.32}$/C	25	C	67	S4
$Pt_{0.67}Ni_{0.33}$/C	25	C	81	S5
PtPd NPs	25	/	50.02	S6
$Pt_{0.65}Ni_{0.35}$	30	/	44.3	S7
PtAuNi	25	/	496	S8
Pt-CoCu@SiO_2	30	SiO_2	272.8	S9
Pt@MIL-101	RT	MOFs	414	S10
PtCo/PEI-GO	25	graphene derivatives	377.83	S11
PtNi/NiO	30	NiO	1240.3	S12
PtCo@PG	30	nanoporous graphene	461.17	S13
Pt/γ-Al_2O_3	30	Al_2O_3	261	S14
Pt/CeO_2	25	CeO_2	182	S15
$Pt_1Co_2Ni_2$-BOFs	**25**	**supramolecular organic frameworks**	**1490**	**This work**

Reference

1. Qi, X.; Li, X.; Chen, B.; Lu, H.; Wang, L.; He, G. Highly Active Nanoreactors: Patchlike or Thick Ni Coating on Pt Nanoparticles based on Confined Catalysis. *ACS Appl. Mater. Interfaces* **2016**, 8, 1922-1928.
2. Yao, C. F.; Zhuang, L.; Cao, Y. L.; Ai, X. P.; Yang, H. X. Hydrogen Release from Hydrolysis of Borazane on Pt-and Ni-based Alloy Catalysts. *Int. J. Hydrogen Energy*, **2008**, 33, 2462-2467.
3. Cui, X.; Li, H.; Yu, G.; Yuan, M.; Yang, J.; Xu, D.; Hou, Y.; Dong, Z. Pt Coated Co Nanoparticles Supported on N-doped Mesoporous Carbon as Highly Efficient, Magnetically Recyclable and Reusable Catalyst for Hydrogen Generation from Ammonia Borane. *Int. J. Hydrogen Energy* **2017**, 42, 27055-27065.
4. Yang, X. J.; Cheng, F. Y.; Tao, Z. L.; Chen, J. Hydrolytic Dehydrogenation of Ammonia Borane Catalyzed by Carbon

Supported Co Core–Pt Shell Nanoparticles. *J. Power Sources* **2011**, 196, 2785-2789.

5. Yang, X. J.; Cheng, F. Y.; Liang, J. Z.; Tao, L.; Chen, J. Carbon-supported Ni1− x@ Ptx (x= 0.32, 0.43, 0.60, 0.67, and 0.80) Core–shell Nanoparticles as Catalysts for Hydrogen Generation from Hydrolysis of Ammonia Borane. *Int. J. Hydrogen Energy* **2011**, 36, 1984-1990.
6. Xu, Q.; Chandra, M. A Portable Hydrogen Generation System: Catalytic Hydrolysis of Ammonia–borane. *J. Alloys Compd.* **2007**, 446-447, 729-732.
7. Yang, X.; Cheng, F.; Liang, J.; Tao, Z.; Chen, J. PtxNi1− x Nanoparticles as Catalysts for Hydrogen Generation from Hydrolysis of Ammonia Borane. *Int. J. Hydrogen Energy* **2009**, 34, 8785-8791.
8. Kang, J.-X.; Chen, T.-W.; Zhang, D.-F.; Guo, L. PtNiAu Trimetallic Aanoalloys Enabled by a Digestive-assisted Process as Highly Efficient Catalyst for Hydrogen Generation. *Nano Energy* **2016**, 23, 145-152.
9. Ge, Y.; Shah, Z. H.; Lin, X. -J.; Lu, R.; Liao, Z.; Zhang, S. Highly Efficient Pt Decorated CoCu Bimetallic Nanoparticles Protected in Silica for Hydrogen Production from Ammonia–Borane. *ACS Sustainable Chem. Eng.* **2017**, 5, 1675-1684.
10. Aijaz, A.; Karkamkar, A.; Choi, Y. J.; Tsumori, N.; Roennebro, E.; Autrey, T.; Shioyama, H.; Xu, Q. Immobilizing Highly Catalytically Active Pt Nanoparticles inside the Pores of Metal–organic Framework: a Double Solvents Approach. *J. Am. Chem. Soc.* **2012**, 134, 13926-13929.
11. Li, M.; Hu, J.; Chen, Z.; Lu, H. A High-performance Pt–Co Bimetallic Catalyst with Polyethyleneimine Decorated Graphene Oxide as Support for Hydrolysis of Ammonia Borane. *RSC Adv.* **2014**, 4, 41152-41158.
12. Ge, Y.; Ye, W.; Shah, Z.H.; Lin, X.; Lu, R.; Zhang, S. PtNi/NiO Clusters Coated by Hollow Sillica: Novel Design for Highly Efficient Hydrogen Production from Ammonia–Borane. *ACS Appl. Mater. Interfaces* **2017**, 9, 3749-3756.
13. Ke, D.; Wang, J.; Zhang, H.; Li, Y.; Zhang, L.; Zhao, X.; Han, S. Fabrication of Pt–Co NPs Supported on Nanoporous Graphene as High-efficient Catalyst for Hydrolytic Dehydrogenation of Ammonia Borane. *Int. J. Hydrogen Energy* **2017**, 42, 26617-26625.
14. Chandra, M.; Xu, Q. Room Temperature Hydrogen Generation from Aqueous Ammonia-borane using Noble Metal Nano-clusters as Highly Active Catalysts. *J. Power Sources* **2007**, 168, 135-142.
15. Wang, X.; Liu, D. P.; Song, S. Y.; Zhang, H. J. Synthesis of Highly Active Pt–CeO2 Hybrids with Tunable Secondary Nanostructures for the Catalytic Hydrolysis of Ammonia Borane. *Chem. Commun.* 2012, 48, 10207-10209.